Mutagen resistance and mutation restriction of St. Louis encephalitis virus

Sara B. Griesemer,[1] Laura D. Kramer,[1,2] Greta A. Van Slyke,[1] Janice D. Pata,[1,2] David W. Gohara,[3] Craig E. Cameron[4] and Alexander T. Ciota[1,2,*]

Abstract

The error rate of the RNA-dependent RNA polymerase (RdRp) of RNA viruses is important in maintaining genetic diversity for viral adaptation and fitness. Numerous studies have shown that mutagen-resistant RNA virus variants display amino acid mutations in the RdRp and other replicase subunits, which in turn exhibit an altered fidelity phenotype affecting viral fitness, adaptability and pathogenicity. St. Louis encephalitis virus (SLEV), like its close relative West Nile virus, is a mosquito-borne flavivirus that has the ability to cause neuroinvasive disease in humans. Here, we describe the successful generation of multiple ribavirin-resistant populations containing a shared amino acid mutation in the SLEV RdRp (E416K). These E416K mutants also displayed resistance to the antiviral T-1106, an RNA mutagen similar to ribavirin. Structural modelling of the E416K polymerase mutation indicated its location in the pinky finger domain of the RdRp, distant from the active site. Deep sequencing of the E416K mutant revealed lower genetic diversity than wild-type SLEV after growth in both vertebrate and invertebrate cells. Phenotypic characterization showed that E416K mutants displayed similar or increased replication in mammalian cells, as well as modest attenuation in mosquito cells, consistent with previous work with West Nile virus high-fidelity variants. In addition, attenuation was limited to mosquito cells with a functional RNA interference response, suggesting an impaired capacity to escape RNA interference could contribute to attenuation of high-fidelity variants. Our results provide increased evidence that RNA mutagen resistance arises through modulation of the RdRp and give further insight into the consequences of altered fidelity of flaviviruses.

INTRODUCTION

St. Louis encephalitis virus (SLEV) is a mosquito-borne member of the genus *Flavivirus*, family *Flaviviridae*, and, like its close relative West Nile virus (WNV), has the ability to cause neuroinvasive disease in humans. These viruses are maintained in transmission cycles between *Culex* mosquitoes and birds, with humans acting as dead-end hosts. Prior to the introduction of WNV in North America in 1999, SLEV was the major cause of epidemic encephalitis by an arbovirus in the USA [1, 2].

All flaviviruses contain a single-stranded, positive-sense RNA genome of approximately 11 kb, encoding a single polyprotein consisting of structural proteins including capsid (C), premembrane (prM) and envelope (E) and nonstructural proteins (NS1, NS2A, NS2B, NS3, NS4A, NS4B, NS5), with additional 5′ and 3′ UTRs. The NS5 encodes two enzymatic domains, including the methyltransferase (MTase) domain at the N-terminus and the RNA-dependent RNA polymerase (RdRp) at the C-terminus [3], which is directly responsible for replication of the viral genome [4]. Due to lack of proofreading ability, RNA viruses containing RdRps have a high intrinsic error rate; approximately 1 mutation per 10 000 nucleotides copied [5] or, in the context of SLEV, ~1 error per genome copied. This high error rate, i.e. low-fidelity RdRp, together with high replication rates, produces a diverse intrahost population of genetically related but heterogeneous variants collectively referred to as the 'mutant swarm' [6]. Intrahost genetic diversity has been hypothesized to allow flaviviruses to rapidly adapt to new environments and evolve resistance to antiviral drugs, as well as contribute to viral fitness and virulence [7–14].

Ribavirin is a compound that has been shown to exhibit antiviral activity against many RNA and DNA viruses, both *in vitro* and *in vivo* [15]. Ribavirin triphosphate, the primary metabolite form of ribavirin, enters the virus's host cell and acts as a nucleoside analogue that is incorporated into viral genomes during RNA synthesis. Because of its ability to pair with both uracil and cytosine, ribavirin triphosphate has been shown to cause transition mutations in replicating genomes. Ribavirin is primarily known to exert antiviral activity by increasing the error rate of viral genome replication, resulting in an accumulation of lethal mutations and consequently a dramatic reduction in infectious viral progeny due to error catastrophe [16]. Previous studies have demonstrated that subjecting a virus to sublethal concentrations of ribavirin can select for ribavirin-resistant variants characterized by increased polymerase fidelity [17–22].

A number of studies with high-fidelity variants of enteroviruses [23–25], as well as recent work with chikungunya virus [19] and WNV [22], demonstrate that decreases in mutation rate are often associated with decreased fitness and pathogenesis in single-host systems. A diminished ability to produce diverse mutant swarms could be particularly detrimental to arboviruses given the requirement for infection, replication and transmission within and between disparate tissues and distinct hosts. Differences in host requirements and/or mutational robustness likely make the cost of altered fidelity both virus and host specific. Investigations of genetic diversity in SLEV and WNV have led to observations that SLEV has a relatively reduced capacity to maintain intrahost diversity [26, 27] and that this reduced diversity could have direct consequences on SLEV adaptability and host range [8].

Studies presented here were designed with the goal of investigating the unique phenotypic and genotypic characteristics of mutagen-resistant SLEV. The generation of multiple ribavirin-resistant SLEV populations with a shared amino acid mutation in the RdRp (E416K) is described. Genetic, phenotypic and structural characterization of these variants provides additional evidence that mutagen-resistant populations develop through dynamic modulation of the RdRp and gives further insight into the mechanism and consequences of altered polymerase fidelity of flaviviruses.

RESULTS

Generation of SLEV with reduced ribavirin susceptibility

Susceptibility of wild-type SLEV-IC to ribavirin in baby hamster kidney (BHK) cell culture was determined prior to passaging (Fig. 1a). SLEV-IC was sequentially passaged eight times on BHK cells, in two parallel lineages, with each lineage passaged in the absence or presence of both 250 and 500 µM ribavirin (Fig. 1b) Infectious titres after growth in each concentration were used to determine which progeny viruses were used for the subsequent passage, with the goal of exerting the maximum selective pressure (ribavirin concentration) while also producing sufficient viral load for the

subsequent passage. Treatment with 500 µM at passages 1–3 resulted in titre reductions from $\sim$4 $\log_{10}$ p.f.u. ml^{-1} after the first passage to $\sim$2.5 $\log_{10}$ p.f.u. ml^{-1} after passage 3 (Fig. 2a). Inocula for these passages were therefore taken from harvests grown in the presence of 250 µM. By passage 4, infectious titre reduction decreased to just over 1 $\log_{10}$ p.f.u. ml^{-1}. As a result, inoculum for passage 5 (and subsequent passages) was taken from growth in the presence of 500 µM. Continued passaging in the presence of 500 µM ribavirin displayed accumulation of resistance in both lineages, as shown by both a reduced reduction relative to the SLEV-IC and an overall decrease in susceptibility compared to earlier passages. By passage 6, a high level of resistance was obtained, particularly for lineage A, for which no measurable effect of ribavirin was evident using this methodology. Increased pretreatment time (1–4 h) was subsequently utilized in an attempt to select for greater resistance; however, decreased resistance was apparent in both populations for passages 7 and 8 (Fig. 2a).

Ribavirin resistance screen of plaque-purified populations

The decreased resistance to ribavirin measured in passage 8 populations (Fig. 2a) was likely due to the altered methodology, yet we assumed resistant variants were likely to still be present in the population. In an attempt to identify mutants associated with resistance, we therefore isolated 10 individual biological clones (plaques) from each population; 6A, 6B, 8A and 8B. Of these 40 biological clones, 36 were successfully amplified on BHK cells (20 from passage 6; 16 from passage 8). Ribavirin resistance screens of all 36 clones in BHK cells identified 12 individual populations with statistically reduced ribavirin susceptibility as compared to SLEV-IC (*t*-test, *P*<0.05); 1 from passage 6B, 5 from passage 8A and 6 from passage 8B. Of these 12 clones, 7 were chosen for sequence analysis and further characterization (Fig. 2b): 1 clone from 6B (clone 6) and 3 each of the most resistant populations, 8A and 8B (clones 2, 3 and 6 and clones 6, 9 and 10, respectively). Despite the lack of significantly resistant clones identified in 6A, the clone from this population that demonstrated the lowest ribavirin susceptibility (clone 9) was included in downstream characterization in order to obtain representative viruses from all populations.

Assessment of mutagen resistance with other systems

To demonstrate that accumulated resistance in BHK cells was due to the selection of ribavirin-resistant viral mutants rather than BHK adaptation, ribavirin susceptibility of the clones demonstrating the highest level of resistance on BHK cells was determined on HeLa cells, which are known to readily take up ribavirin [18, 28]. Treatment with 100 µM ribavirin resulted in significantly lower reduction in infectious titres of 6B-6, 8B-6 and 8B-9 relative to SLEV-IC at 72 h post-infection (p.i.) (Fig. 3a; *P*≤0.05, Student's *t*-test). As with BHK experiments, the most resistant clone was determined to be 8B-9.
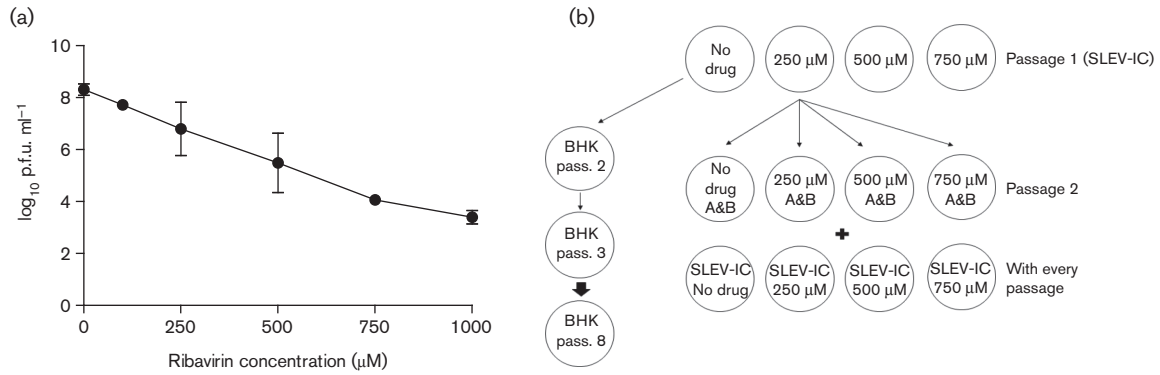
Fig. 1. Initial characterization and experimental design. (a) Susceptibility of SLEV-IC to ribavirin on BHK cells. BHK cells were pretreated with maintenance media containing 0, 250, 500, 750 or 1000 µM ribavirin for 1 h. Infections were done at a m.o.i. of 0.01, and viral titres were assessed in triplicate assays at 72 h p.i. and depicted as mean±SD (b) Schematic of SLEV serial passage in BHK cells to create ribavirin resistance. Duplicate wells were infected with SLEV-IC and deemed lineages A and B throughout passaging. Infectious titres were determined with and without ribavirin treatment following 72 h growth for each passage and compared to the unpassed SLEV-IC control. Treated viruses were passaged again in BHK cells with multiple concentrations of ribavirin.

Viral variants exhibiting resistance to ribavirin are likely to be higher-fidelity variants [18, 20, 29], yet lethal mutagenesis is just one of many identified antiviral mechanisms of ribavirin [30–33]. To determine if ribavirin-resistant variants showed resistance to other mutagens (therefore implicating altered fidelity in decreased susceptibility), two of the most resistant viruses, 6B-6 and 8B-9, were subjected to treatment with T-1106, a recently developed antiviral drug for treatment of RNA virus infections [34]. Initial treatment with T-1106 demonstrated that wild-type SLEV is sensitive to the drug in BHK cells, with a >3 $\log_{10}$ reduction in

infectious titre with 100 µM treatment (Fig. 3b). Both 6B-6 and 8B-9 viruses displayed significantly reduced sensitivity to T-1106 after treatment with 100 µM, as compared to the wild-type control (Fig. 3b). Decreased susceptibility to both T-1106 and ribavirin suggests a broad mechanistic basis consistent with increased RdRp fidelity.

NS5 sequencing

Sequencing of the complete NS5 gene from parental populations (6A, 6B, 8A, 8B) and ribavirin-resistant clones (Fig. 2b) was performed to identify point mutations with a
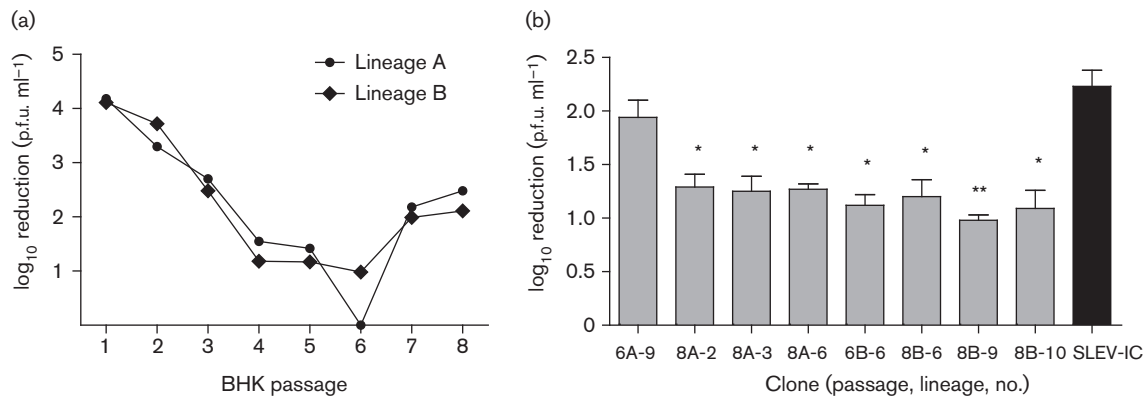
Fig. 2. Selection of SLEV with reduced ribavirin susceptibility. (a) Serial passage of SLEV in BHK cells in the presence of ribavirin. $\log_{10}$ reduction in infectious titre refers to the log difference between infectious titres with and without treatment. At each passage, viruses were subjected to 250 and 500 µM ribavirin. The response to 500 µM ribavirin throughout the passage experiment is shown. Inocula for passages 2–4 were taken following treatment with 250 µM and passages 5–8 following treatment with 500 µM ribavirin. The pretreatment period was increased from 1 to 4 h for passages 7 and 8. (b). Ribavirin susceptibility of selected clones. Graph represents the mean overall difference in infectious titre of each clone (mean reduction ±SD), after treatment with two concentrations (250 and 500 µM) of ribavirin and growth on BHK cell culture, as compared to infectious titre obtained after growth of same clone without ribavirin. Significance is determined by Student's *t*-test as compared to mean overall reduction obtained with the SLEV-IC control. *$P \leq 0.05$, **$P < 0.01$.
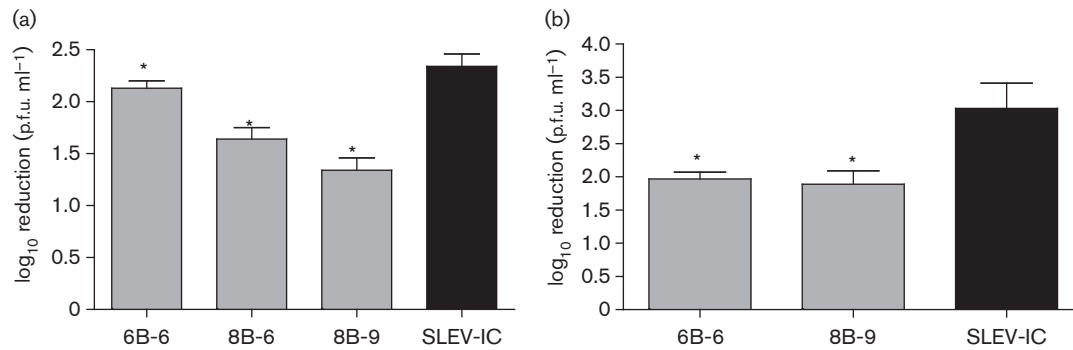
Fig. 3. Resistance is not host cell or mutagen dependent. (a) Ribavirin susceptibility of selected clones on HeLa cells. Cells were pretreated and held with or without 100 µM ribavirin, in triplicate, following infection at a m.o.i. of 0.01, and harvested 3 days p.i. Reduction in titre was determined by subtracting titre obtained in the presence of ribavirin from the titre obtained without drug. (Mean viral reduction±SD is shown; *P≤0.05, Student's *t*-test). (b) T-1106 susceptibility of selected clones on BHK cells. Cells were pretreated and held with or without 100 µM T-1106, in triplicate, following infection at a m.o.i. of 0.01, and harvested 3 days p.i. Reduction in titre was determined by subtracting titre obtained in the presence of ribavirin from the titre obtained without drug. (Mean viral reduction±SD is shown; *P≤0.05, Student's *t*-test).

putative role in mutagen susceptibility and/or RdRp fidelity. A total of 30 mutations were identified in these variants, including 9 nonsynonymous mutations resulting in residue changes in both the MTase and RdRp domains of the NS5 (Table 1; GenBank accession no. KY271950–53). Interestingly, passage 6B parental population and five of the eight clones displayed a single shared mutation at nucleotide position 8916 of the genome (G8916A), resulting in a glutamic acid-to-lysine change at residue 416 of the RdRp (E416K). Of these five clones, one represented lineage A and the other four represented lineage B, demonstrating parallel acquisition of this mutation. Further analysis of sequence chromatograms showed evidence of a minority population of G8916A in passage 6A, 8A and 8B parental viruses, indicated by smaller secondary A peaks at the 8916 position. No other nonsynonymous mutations were shared among resistant populations. In addition, no nonsynonymous mutations were identified in the untreated,

BHK-passaged populations, as compared to the SLEV-IC, suggesting that the NS5 changes observed in the treated populations were most likely due to ribavirin pressure rather than adaptation to BHK cells.

Molecular modelling and mapping of E416K

Based on the highly resolved crystal structure of the full-length NS5 protein from Japanese encephalitis virus (JEV) [35], the E416K mutation is located in motif G, or the pinky domain, of the RdRp, distant from the active site of the enzyme (Fig. 4). This residue has physical proximity to the structurally conserved residues (410 and 411) of the pinky domain known to interact with the +1/+2 junction of the RNA template strand and, based on its position in the incoming RNA template channel, could also interact with the template strand. Superimposition of the JEV NS5 with a crystal structure of the RNA primer–template complex from HCV NS5B [35, 36] suggests that this interaction is

Table 1. Observed NS5 amino acid substitutions in SLEV ribavirin-resistant variants

Mutation*	Amino acid†	Variants	NS5 domain
C7867T	T66I	8B-10	MTase
C7992T	P108L	8A-2	MTase
C8197T	A176V	8A-2	MTase
G8343A	A225T	8B-10	MTase
G8346A	A226T	8A-6	MTase
A8889G	S407G	8A-6	RdRp
G8916A	E416K	6A‡, 6B, 6B-6, 8A‡, 8A-2, 8A-3, 8A-6, 8B‡, 8B-6, 8B-9, 8B-10	RdRp
G9567A	D633N	8A-6	RdRp
T9583C	M638T	8A-6	RdRp

*Nucleotide position of complete genome of SLEV, Imperial Valley strain, GenBank accession no. JF460774.

†Amino acid residue position of SLEV NS5 gene, GenBank accession no. AEN02430.

‡Evidence of mixed populations observed in sequence chromatograms of parental sample.

Fig. 4. Structure of the NS5 protein with SLEV-E416K. The MTase domain (cyan) and polymerase domain (blue) are shown in ribbon form looking into the active site. Residue E416 is displayed as space-filling spheres (red), and the catalytic GDD sequence (motif C) is in stick representation (magenta).

likely. Bases +1, +0, −1 and −2 from the template strand are ordered in the crystal structure, with the +2 base only showing an ordered backbone. Despite this disorder, it is clear that the sugar and phosphate of this +2 residue are positioned up the RNA template entrance tunnel (in close proximity with A410 and A411), and residue 416 is likely to interact with residues of the template at the +3 or +4 upstream position.

In vitro growth kinetics of ribavirin-resistant viruses

To investigate possible alterations to replicative fitness associated with ribavirin resistance in different hosts, growth kinetics of four clones (6B-6, 8B-6, 8B-9, 6A-9), including the most resistant clones, were assessed in mammalian (BHK and HeLa) and mosquito (CxT) cells, and overall mean and peak titres were compared to SLEV-IC. All variants replicated to higher peak titres than SLEV-IC in BHK cells (t-test, $P<0.05$), and reached peak titre sooner (48 vs 72 h, Fig. 5). With the exception of 6A-9, this increased replicative fitness was also measured on HeLa cells. Growth kinetics in invertebrate cells was more variable, with variants demonstrating either statistically similar or attenuated growth. However, 6B-6 and 6A-9 replicated to significantly lower overall mean titres (paired t-test, $P<0.05$), and 6B-6, 6A-9 and 8B-9 had lower peak titres relative to SLEV-IC (t-test, $P<0.05$; Fig. 5).

In order to assess how the lack of a functional RNA interference (RNAi) response influenced viral replication [37], peak viral load following growth on C6/36 cells was quantified and compared to viral load following growth on CxT cells.

Despite attenuation on CxT cells for three of the four SLEV clones, all variants grew to similar titres to SLEV-IC on C6/36 cells (Fig. 6).

Population diversity analysis

To investigate how a mutagen-resistant variant containing the E416K polymerase mutation differs in its capacity to generate genetic diversity, mutation frequencies of an approximately 3 kb region of SLEV-IC and 8B-9 were evaluated by deep sequencing after a single passage in BHK and C6/36 cells. To ensure that viruses had gone through the same number of replication cycles and mutation frequencies could therefore be compared to make accurate inferences about error rates, sequencing was completed for virus populations isolated at 72 h p.i., when SLEV-IC and 8B-9 had statistically similar titres (Figs 5 and 6). Both populations sequenced contained numerous low-frequency variants (<1 %) distributed throughout the 3 kb region, in both cell lines. However, more positions across the SLEV-IC genome displayed mutation frequencies above 1 % as compared to the 8B-9 virus (12 vs 3), and calculation of the overall alternate allele frequency of the SLEV-IC was significantly higher than 8B-9 in both BHK and C6/36 cells (Fig. 7; Mann–Whitney U test, $P<0.001$; 7.8×10^{-4} vs 6.7×10^{-4} and 8.6×10^{-4} vs 7.2×10^{-4}, respectively), consistent with a modest decrease in 8B-9 mutation frequency relative to SLEV-IC.

DISCUSSION

Alteration of the replication complex of RNA viruses can give insight into how the structure and function of these proteins affect viral fitness, adaptability and pathogenesis in their respective hosts [19–22, 38–41]. Our results are consistent with past studies and give further evidence that modest biochemical alterations in viral RdRps can not only confer mutagen resistance but also slow the accumulation of intrahost genetic diversity and ultimately have profound effects on viral fitness and evolution. Generation of a ribavirin-resistant SLEV was successful after six passages in BHK with ribavirin treatment. The increased mutagen susceptibility beyond passage 6 was not necessarily surprising. It has been shown that cellular uptake of ribavirin and availability for viral genome incorporation increases as pretreatment time increases [28, 42], so the additional pretreatment time at passages 7 and 8 presumably amplified the amount of available ribavirin in the cells and therefore increased the mutagenic effect. In addition, although more resistant strains are presumably producing less genetic diversity, deleterious mutants continue to accumulate in the presence of ribavirin. As a result, one can assume that infection of each passage was completed with populations of increasing diversity and therefore populations that are theoretically closer to the error threshold.

As predicted, sequence analysis of the viruses used in this study indicated that ribavirin-resistant populations acquired amino acid changes in the RdRp that were not present in untreated populations (Table 1). In fact, a single shared
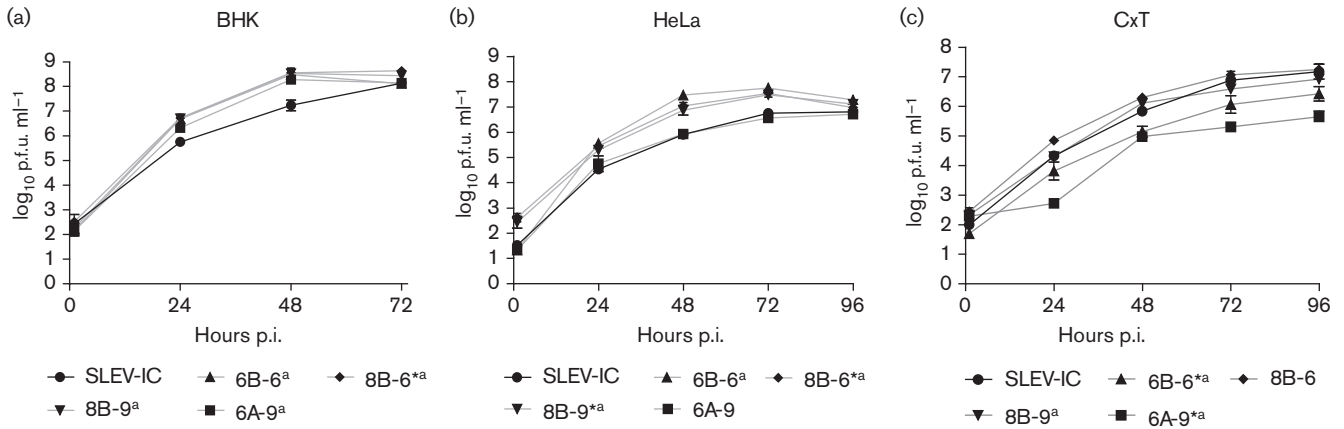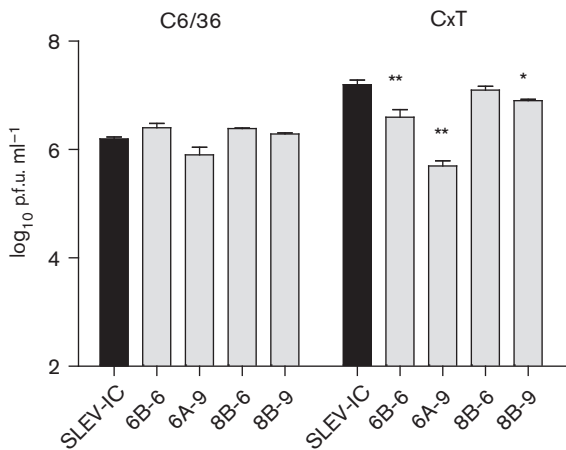
Fig. 5. *In vitro* growth kinetics of ribavirin-resistant SLEV clones in vertebrate and invertebrate cell lines. Cells were inoculated in triplicate at a m.o.i. of 0.01. Supernatant titres were determined by plaque assay on Vero cells. Mean titres±SD are shown. *$P<0.05$, paired *t*-test, as compared to the SLEV-IC. [a]Peak titre, $P<0.05$, *t*-test as compared to the SLEV-IC.

mutation in the RdRp (E416K) was identified in the consensus sequences of five of the eight individual populations analysed and one of the parental populations. Although not observed as a consensus change, evidence of the mutation was also present in minor populations of the other three parental populations, explaining why all of the biological clones studied did not contain the E416K mutation. The identification of this RdRp mutation in ribavirin-resistant viruses from both lineages, exclusively in mutagen-treated viruses, and as the only mutation identified within the NS5 protein of the most resistant clone, 8B-9, suggests that this residue is an important mediator of resistance. In addition,

Fig. 6. Lack of attenuation of ribavirin-resistant SLEV clones in mosquito cells lacking a functional RNAi response. Cells were inoculated in triplicate at a m.o.i. of 0.01 and harvested at 96 h p.i. Supernatant titres were determined by plaque assay on Vero cells. Mean titres±SD are shown. Significantly lower viral loads relative to SLEV-IC (*$P<0.05$, **$P<0.01$, paired *t*-test) were identified in three of four SLEV variants in CxT but not C6/36 cells.

the loss of the E416K mutation from a consensus mutation in passage 6B (increased resistance) to a minority population in passage 8B (reduction in resistance) lends further support to its role.

Mapping of the SLEV E416K mutation using the highly resolved JEV NS5 crystal structure indicated that it is positioned in the pinky domain distant from the known active site of the enzyme, a characteristic that is common among mutagen-resistant viruses [43]. Improved structural data of this domain indicated that the pinky finger is bulkier than the other fingers, forms one side of the dsRNA channel and, because of its structural conservation among other flaviviruses, most likely plays an important role in RdRp–RNA complex stability as well as RdRp movement along the RNA template strand [35]. The replacement of glutamic acid with lysine (negative to positive charge) could presumably perturb fidelity by altering the affinity of the RdRp for the RNA template, yet given the dynamic nature of these interactions, an accurate understanding of the biochemical mechanism here would require complex enzymatic assays utilizing wild-type and mutant RdRps and their subunits. While the E416K mutation is located in the SLEV pinky domain and the high-fidelity mutations previously identified in WNV are located in the priming loop and thumb domain, all these residues are predicted to have some impact on complex stability [22]. These results add to the growing body of evidence that residues remote from the active site can have significant effects on replicase function.

The E416K mutation is the only shared NS5 amino acid change among the resistant clones; however, four additional residues in the RdRp and five residues in the MTase region were identified. A recent study with WNV was the first to directly identify a role for the MTase in mutagen resistance and clearly demonstrates that altered replicase subunit interactions can have a profound effect on polymerase
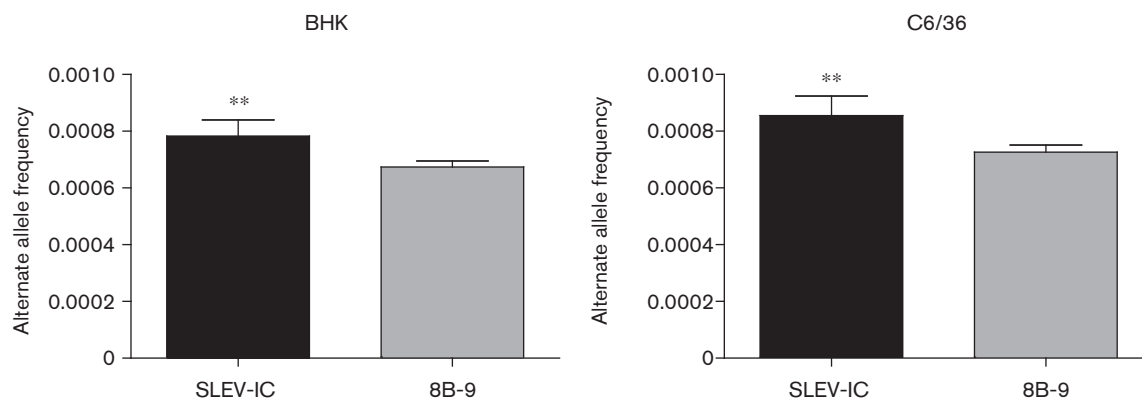
Fig. 7. Decreased mutation frequency of 8B-9 relative to SLEV-IC. Mean alternate allele frequency of SLEV-IC and 8B-9 in BHK and C6/36 cells±SEM across the sequenced genome (~3000 bp). Alternate allele refers to any base call other than that of the majority consensus. Significantly higher frequencies were measured for SLEV-IC in both cell lines relative to SLEV 8B-9 (**Mann–Whitney *U* test, $P < 0.001$).

fidelity [22]. The mutations identified here provide additional support for the role of the flavivirus MTase and further demonstrate that accurate and comprehensive evaluation of RdRp function and fidelity requires considerations of interactions among replicase subunits. Although the goal of this study was to investigate the potential function of the SLEV NS5 in mutagen resistance and mutation restriction, it is also possible that mutations outside of the NS5, particularly the helicase portion of the NS3, alter RdRp function allosterically and/or protect against other mechanisms of antiviral action.

The antiviral T-1106 is a pyrazine derivative structurally related to T-705 (favipiravir) and designed to specifically target the viral RdRp without affecting host-cell DNA or RNA synthesis [44, 45]. Recently, T-705 has been shown to exert its antiviral effects through induction of lethal mutagenesis in influenza viruses [46], suggesting that these pyrazine derivatives may act as base analogues similar to ribavirin. Studies of these compounds have demonstrated antiviral activity against many RNA viruses *in vivo*, including the flaviviruses WNV and yellow fever virus [34]. We have demonstrated that not only is T-1106 effective against wild-type SLEV *in vitro* but ribavirin-resistant variants also acquired resistance to T-1106, adding more support to the hypothesis that the mutations conferring resistance likely modulate fidelity of the viral RdRp.

The observation of decreased intrahost diversity of 8B-9 in both BHK and C6/36 cells, as compared to the wild-type, further supports the notion that 8B-9 possesses a higher-fidelity phenotype most likely conferred by E416K. The alternate allele frequencies observed across the genome were within the range of what would be expected for RNA polymerase error rates, yet the use of a high-fidelity polymerase amplification, the combined error rates of the reverse transcriptase, the DNA polymerase and the Illumina MiSeq technology together make it difficult to distinguish amplification and sequencing errors

from true low-frequency variants. Nonetheless, the experimental methods for amplification, library preparation, sequencing and analysis were identical for all samples, and thus it can be assumed that there was no error bias for any specific sample and that comparison of overall variant frequencies is therefore an accurate reflection of relative differences in viral mutation frequencies.

Recent studies with chikungunya virus antimutator and mutator variants reported that increased mutation frequency seen with mutator variants in mammalian cells was negated in mosquito cells and mutation frequency of the wild-type and mutator variants was lower in mosquito cells as compared to mammalian cells [38]. In contrast, analyses of 8B-9 presented here show lower mutation frequencies in both mammalian and mosquito cells relative to SLEV-IC and higher mutation frequencies of both SLEV-IC and 8B-9 in mosquito cells as compared to vertebrate cells. The more diverse mutant swarms in mosquito cells are consistent with previous studies indicating that genetic diversity is well tolerated and possibly selected for in the mosquito host [6, 9, 13, 47, 48]. Together, these studies demonstrate that mutational frequencies are likely both virus and host dependent.

Van Slyke *et al*, found that increased fidelity of WNV resulted in equivalent replicative fitness in vertebrate cells and a modest attenuation in mosquito cells [22]. Consistent with this, mutagen-resistant SLEV demonstrated either similar kinetics or a replicative advantage in vertebrate cells, as well as equivalent kinetics or modest attenuation in mosquito cells. The increased viral titres in vertebrate cells are likely due to adaptive mutations that are independent of NS5 mutations, consistent with previous studies with SLEV demonstrating cell-specific adaptation *in vitro* [27, 49]. Although it is possible that any fitness costs induced by altered RdRp function in mammalian cells may be overcome by compensatory adaptive mutations, these results generally support the idea that viral fitness in vertebrate cells is not significantly impaired by

increased RdRp fidelity. As has been shown in other systems [17, 19, 41, 50], decreases in virulence and/or kinetics *in vivo* are not always reflected by *in vitro* kinetics, so future experimentation with animal models could reveal additional phenotypic alterations.

The loss of replicative fitness of multiple variants in mosquito cells, although consistent with previous studies of fidelity variants [19, 22], could also be explained by phenotypic trade-offs resulting from adaptation to BHK cell culture. Although host specialization does not consistently result in a phenotypic cost in divergent cell lines, studies with mosquito-cell-adapted SLEV did document a fitness cost in vertebrate cell culture with some strains [8, 27], and such trade-offs have also been documented with other arboviruses following adaptation to BHK cells [51, 52]. Taken together, studies with WNV in both mosquitoes and cell culture demonstrate a correlation between genetic diversity and viral fitness and suggest that this could be tied to the capacity to effectively evade the invertebrate RNAi response [7, 47, 53]. It is logical that a decreased capacity to produce mutations would hinder the ability of a virus to evade a response that relies on precise sequence recognition. Our results support this. Specifically, we demonstrate that ribavirin-resistant variants that are attenuated in CxT cells are not attenuated in C6/36 cells, which lack a functional RNAi response. Further studies characterizing how the extent and specificity of RNAi responses compare among infections with variants possessing altered replicase function are needed to fully understand this relationship. Furthermore, comprehensive assessment of the influence of E416K and other mutations will ultimately require the creation and utilization of SLEV reverse-genetics systems. Such studies will help to elucidate the role and mechanism of the flavivirus replication complex in viral fitness and adaptation.

METHODS

Cells and viruses

African green monkey kidney cells (Vero, ATCC), BHK cells (BHK-21, ATCC) and human cervical cancer cells (HeLa, ATCC) were grown in EMEM supplemented with 10 % (v/v) FBS, 2 mM L-glutamine, 1.5 g l^{-1} sodium bicarbonate, 100 U ml^{-1} penicillin and 100 µg ml^{-1} streptomycin. *Aedes albopictus* mosquito cells (C6/36, ATCC no. CRL-1660) were grown in MEM supplemented with 10 % (v/v) FBS, 2 mM L-glutamine, 1.5 g l^{-1} sodium bicarbonate, 0.1 mM non-essential amino acids, 100 U ml^{-1} penicillin and 100 µg ml^{-1} streptomycin. *Culex tarsalis* mosquito cells (CxT), originally from University of California Davis and kindly provided by A. Brault (Centers for Disease Control andPrevention Fort Collins), were grown in Schneider's insect medium (Sigma) supplemented with 10 % (v/v) FBS. Mammalian cells were grown and maintained at 37 °C in 5 % CO$_2$, and mosquito cells, at 28 °C in 5 % CO$_2$.

Wild-type SLEV-IC was previously generated in the arbovirus laboratory using an infectious cDNA clone kindly provided by A. Brault (Centers for Disease Control and Prevention Fort Collins). This clone was originally created from SLEV strain IMP115, isolated from a pool of *C. tarsalis* mosquitos from Imperial Valley, CA, in 2003. Virus was rescued in BHK cells using a two-plasmid reverse-genetics system as previously described [54]. In order to keep population diversity at a minimum and directly compare ribavirin effects in the absence of other contributing factors, such as host adaptation and increased diversity due to passaging, rescued virus amplified once on BHK cells was used as the starting stock virus in ribavirin selection and subsequent characterizations.

Mutagen passage and creation of ribavirin resistance

SLEV-IC was passaged eight times in six-well plates seeded with BHK cells, in the presence or absence of ribavirin, and harvested 3–4 days p.i. (Fig. 1). Cells were pretreated with maintenance media (with either no drug) or 250 or 500 µM ribavirin (Sigma) for 1 h (pass. 1–6) or 4 h (pass. 7 and 8), incubated with virus for 1 h at 37 °C, washed and overlaid with fresh media with the same concentrations of ribavirin. Each passage experiment contained a fresh untreated, unpassaged SLEV-IC control, which was subjected to ribavirin treatment, as well as an untreated, BHK-passaged virus. For the first passage, virus was inoculated at a m.o.i. of 0.1 into duplicate wells, each assigned as a separate lineage (A and B) throughout the passage experiments. Infectious titres were measured by Vero cell plaque assay after each passage and used to determine which progeny virus population, i.e. grown in the presence of 250 or 500 µM ribavirin, to use for infection of each subsequent passage. To provide adequate selective pressure without lethality, the concentration that reduced viral populations approximately 2 logs, but not more than 2 logs, was chosen for the next passage. Inocula for passages 1–4 were from growth in 250 µM ribavirin, followed by 500 µM inocula for passages 5–8. The m.o.i. ranged from 0.001 to 0.1 with passages 1–4 and, as resistance developed and titres increased in treated viruses, was consistently 0.01 with passages 5–8. Reductions in titre resulting from ribavirin treatment were compared at each passage for both lineages and the SLEV-IC. This was performed by subtracting the viral titre observed with treatment from the titre observed without treatment.

Plaque isolation

Harvested parental populations from passages 6A, 6B, 8A and 8B were serially diluted to concentrations that produced between 10 and 50 well-separated plaques and inoculated onto confluent BHK cell monolayers for standard plaque assay. Ten distinct plaques were picked from each passage and lineage, and the agarose plug was transferred to 250 µl EMEM + 20 % (v/v) FBS and frozen for further analysis. To create a larger stock for downstream studies, 100 µl of purified plaque sample was amplified once in BHK cells and titrated by Vero cell plaque assay. The remaining sample was used for RNA purification and sequencing.

Viral growth kinetics

Six-well plates containing confluent monolayers of BHK, HeLa and CxT cells were infected with virus, in triplicate, at a m.o.i. of 0.01. Virus was allowed to adsorb to the cells for 1 h at 37 °C (BHK and HeLa) or 28 °C (CxT), after which the inoculum was removed and wells were washed with maintenance media and replaced with 3 ml maintenance media. Supernatant (50 µl) was taken from each well at 1, 24, 48, 72 and 96 h p.i. All samples were diluted 1 : 10 with EMEM + 20 % (v/v) FBS and frozen at −80 °C. Samples were titrated by Vero cell plaque assay as previously described [55], in duplicate, with six-well plates and averaged. Growth curves were plotted using the triplicate geometric mean titre and SD ($\log_{10}$ p.f.u. ml^{-1}) for each time point.

NS5 amplification and sequencing

A total of 24 samples were chosen for sequencing analysis: ribavirin-treated parental populations 6A, 6B, 8A and 8B (at 500 µM ribavirin); BHK serially-passaged, untreated populations 6A, 6B, 8A and 8B; and eight clonal populations from ribavirin-treated parental populations – 6A-9, 6B-6, 8A-2, 8A-3, 8A-6, 8B-6, 8B-9 and 8B-10. Both the unpassaged and BHK-passaged harvests of each of the clones were analysed. RNA was extracted using the QIAamp Viral RNA Mini kit (Qiagen) according to the manufacturer's protocol. The entire NS5 gene was amplified by RT-PCR in four overlapping fragments, each between 1.0 and 1.5 kb, for a total sequence length of approximately 4.8 kb using the Qiagen OneStep RT-PCR kit (primer sequences upon request).

PCRs were visualized by gel electrophoresis and gel purified using the MinElute Gel Extraction kit (Qiagen) when multiple non-specific bands were seen. In instances when only one amplification product was observed, i.e. a single band on the gel, PCR products were purified directly from PCRs using the QIAquick PCR Purification kit.

Multiple primers targeting sequence within each amplicon were used for bidirectional sequencing to create at least two-fold overlapping coverage of the entire NS5 gene (full list available upon request) All sequencing was performed at the Albert Einstein College of Medicine's Genomics Core using an Applied Biosystems 3730 automated sequencer (Life Technologies). Sequences were compiled and edited using the Seq-Man module of the DNAStar software package, version 8.0 (DNAStar). Consensus sequences from samples were aligned and compared to that of the unpassaged, untreated SLEV-IC wild-type sequence using Sequencher (Gene Codes).

Molecular modelling

NS5 crystal structures were obtained from the Research Collaboratory for Structural Bioinformatics Protein Data Bank, modified and superimposed in PyMOL, version 1.8. Due to the lack of available high-resolution SLE NS5 crystal structures, figures were generated from Protein Data Bank entry 4K6M (JEV full-length NS5). To map amino acid changes in ribavirin-resistant populations to the polymerase structure, full-length polyprotein sequences from the SLE

Imperial Valley strain (GenBank accession no. AEN02430) and JEV SA14 strain (GenBank accession no. AAA21436) were aligned with CLUSTALW2 [56].

Mutagen sensitivity

To test the mutagen sensitivity of passages 6A, 6B, 8A and 8B plaque-purified variants to ribavirin, a total of 36 clones, isolated and amplified once in BHK-21 cells, were grown in the presence of different ribavirin concentrations and progeny virus was titred by plaque assay. BHK cells were pretreated with maintenance media containing 0, 250 or 500 µM ribavirin (Sigma R9644) for 1 h (passage 6 clones) or 4 h (passage 8 clones), at 37 °C with 5 % (v/v) CO_2. Pretreatment media was removed, and cells were infected, in duplicate, at a m.o.i. of 0.01. After adsorption for 1 h at 37 °C, inoculum was removed and cells were washed and replaced with maintenance media containing the same ribavirin pretreatment concentration. After 72 h, 1 ml of supernatant was harvested from each well and frozen at −80 °C. Infectious titres ($\log_{10}$ p.f.u. ml^{-1}) were determined by Vero cell plaque assay and averaged. For each drug concentration, mean titres obtained after growth in the presence of ribavirin were subtracted from the mean titre obtained after growth with no drug ($\log_{10}$ p.f.u. ml^{-1} reduction). Reductions in infectious titre obtained with 250 and 500 µM were then averaged to acquire an overall titre reduction. Overall titre reductions were compared to the overall titre reduction of the SLEV-IC wild-type virus by Student's *t*-test. Samples with both a lower reduction in infectious titre and a *P*-value ≤0.05 were defined as having increased resistance to ribavirin. Variants 6B-6, 8B-6 and 8B-9 were also tested for ribavirin resistance in HeLa cells. Cells were pretreated with 0 and 100 µM ribavirin for 1 h, infected at a m.o.i. of 0.01 and harvested 72 h p.i. Infectious titres were compared to those of the SLEV-IC wild-type as described above.

T-1106, a closely related derivative of the RNA mutagen favipiravir (T-705), was kindly provided by D. Harki at the University of Minnesota. T-1106 sensitivity assays were performed similar to ribavirin sensitivity assays. Twelve-well plates, confluent with BHK cells, were pretreated for 1 h with maintenance media containing 0, 100, 200 and 500 µM T-1106. Media was removed, and cells were infected, in triplicate, with SLEV-IC wild-type, ribavirin-resistant 6B-6 and 8B-9. Inoculum was removed, cells were washed and replaced with T-1106-containing media and supernatant was collected 72 h p.i. for infectious titre determination. Comparisons were performed as above.

Population diversity by deep sequencing

Population diversity was estimated by deep sequencing of SLEV-IC and 8B-9, a ribavirin-resistant virus containing only the RdRp E416K mutation in the NS5 gene. Supernatants were taken from the BHK and C6/36 viral growth curve experiments after 72 h p.i.

A 3 kb fragment, spanning a portion of the premembrane (prM) protein, the entire envelope (E), entire non-structural

protein 1 (NS1) and a portion of the non-structural protein 2 (NS2), was amplified by one-step RT-PCR using Invitrogen's Superscript III One-Step RT-PCR System with Platinum *Taq* High Fidelity (Life Technologies). Amplicons were visualized by electrophoresis, gel purified using the MinElute Gel Extraction kit (Qiagen) and sent to Albert Einstein College of Medicine's Epigenetics Core for library preparation and sequencing. PCR amplicons were fragmented, tagged with specific adapters for multiplexing, clustered and sequenced in the same lane using Illumina's MiSeq Desktop Sequencer. Amplicons were sequenced with production of 2×300 bp paired-end reads.

Data analysis was performed by the Wadsworth Center's Applied Genomics Technologies Core. Sequencing read qualities were analysed in FastQC (Babraham Institute, Cambridge, UK, http://www.bioinformatics.babraham.ac.uk/projects/fastqc), trimmed to a maximum of 250 bp to reduce the number of low-quality base calls at the end of the reads and also filtered to contain those at least 150 bp. Reads were mapped and aligned to the reference SLEV-IC sequence with Burrows–Wheeler Aligner MEM [57]. PCR read duplicates were removed using SAMtools rmdup [58], and allele counts and frequencies were calculated from SAMtool mpileups using an in-house perl script.

Statistics

Statistical analyses were performed using both Microsoft Excel (Student's *t*-test) and GraphPad Prism. *P*-values ≤0.05 were considered significant.

Conflicts of interest
The authors declare that there are no conflicts of interest.

References
1. **Monath TP.** Epidemiology. In: Monath TP (editor). *St. Louis Encephalitis*. Washington, DC: American Public Health Association; 1980. pp. 239–312.
2. **Reisen WK.** Epidemiology of St. Louis encephalitis virus. *Adv Virus Res* 2003;61:139–183.
3. **Tan CS, Hobson-Peters JM, Stoermer MJ, Fairlie DP, Khromykh AA** *et al.* An interaction between the methyltransferase and RNA dependent RNA polymerase domains of the West Nile virus NS5 protein. *J Gen Virol* 2013;94:1961–1971.
4. **Zhang B, Dong H, Zhou Y, Shi PY.** Genetic interactions among the West Nile virus methyltransferase, the RNA-dependent RNA polymerase, and the 5′ stem–loop of genomic RNA. *J Virol* 2008;82:7047–7058.
5. **Drake JW, Holland JJ.** Mutation rates among RNA viruses. *Proc Natl Acad Sci USA* 1999;96:13910–13913.
6. **Ciota AT, Jia Y, Payne AF, Jerzak G, Davis LJ** *et al.* Experimental passage of St. Louis encephalitis virus *in vivo* in mosquitoes and chickens reveals evolutionarily significant virus characteristics. *PLoS One* 2009;4:e7876.
7. **Ciota AT, Ehrbar DJ, Van Slyke GA, Willsey GG, Kramer LD.** Co-operative interactions in the West Nile virus mutant swarm. *BMC Evol Biol* 2012;12:58.
8. **Ciota AT, Lovelace AO, Jones SA, Payne A, Kramer LD.** Adaptation of two flaviviruses results in differences in genetic heterogeneity and virus adaptability. *J Gen Virol* 2007;88:2398–2406.
9. **Ciota AT, Ngo KA, Lovelace AO, Payne AF, Zhou Y** *et al.* Role of the mutant spectrum in adaptation and replication of West Nile virus. *J Gen Virol* 2007;88:865–874.
10. **Ebel GD, Fitzpatrick KA, Lim PY, Bennett CJ, Deardorff ER** *et al.* Nonconsensus West Nile virus genomes arising during mosquito infection suppress pathogenesis and modulate virus fitness *in vivo*. *J Virol* 2011;85:12605–12613.
11. **Fan X, Mao Q, Zhou D, Lu Y, Xing J** *et al.* High diversity of hepatitis C viral quasispecies is associated with early virological response in patients undergoing antiviral therapy. *Hepatology* 2009;50:1765–1772.
12. **Fitzpatrick KA, Deardorff ER, Pesko K, Brackney DE, Zhang B** *et al.* Population variation of West Nile virus confers a host-specific fitness benefit in mosquitoes. *Virology* 2010;404:89–95.
13. **Jerzak GV, Bernard K, Kramer LD, Shi PY, Ebel GD.** The West Nile virus mutant spectrum is host-dependant and a determinant of mortality in mice. *Virology* 2007;360:469–476.
14. **Veillon P, Payan C, Gaudy C, Goudeau A, Lunel F.** Mutation analysis of ISDR and V3 domains of hepatitis C virus NS5A region before interferon therapy with or without ribavirin. *Pathol Biol* 2004;52:505–510.
15. **Crotty S, Maag D, Arnold JJ, Zhong W, Lau JY** *et al.* The broad-spectrum antiviral ribonucleoside ribavirin is an RNA virus mutagen. *Nat Med* 2000;6:1375–1379.
16. **Crotty S, Cameron CE, Andino R.** RNA virus error catastrophe: direct molecular test by using ribavirin. *Proc Natl Acad Sci USA* 2001;98:6895–6900.
17. **Vignuzzi M, Stone JK, Arnold JJ, Cameron CE, Andino R.** Quasispecies diversity determines pathogenesis through co-operative interactions in a viral population. *Nature* 2006;439:344–348.
18. **Beaucourt S, Bordería AV, Coffey LL, Gnädig NF, Sanz-Ramos M** *et al.* Isolation of fidelity variants of RNA viruses and characterization of virus mutation frequency. *J Vis Exp* 2011.
19. **Coffey LL, Beeharry Y, Borderia AV, Blanc H, Vignuzzi M.** Arbovirus high fidelity variant loses fitness in mosquitoes and mice. *Proc Natl Acad Sci USA* 2011;108:16038–16043.
20. **Pfeiffer JK, Kirkegaard K.** A single mutation in poliovirus RNA-dependent RNA polymerase confers resistance to mutagenic nucleotide analogs via increased fidelity. *Proc Natl Acad Sci USA* 2003;100:7289–7294.
21. **Sierra M, Airaksinen A, González-López C, Agudo R, Arias A** *et al.* Foot-and-mouth disease virus mutant with decreased sensitivity to ribavirin: implications for error catastrophe. *J Virol* 2007;81:2012–2024.
22. **Van Slyke GA, Arnold JJ, Lugo AJ, Griesemer SB, Moustafa IM** *et al.* Sequence-specific fidelity alterations associated with West Nile virus attenuation in mosquitoes. *PLoS Pathog* 2015;11:e1005009.
23. **Graham RL, Becker MM, Eckerle LD, Bolles M, Denison MR** *et al.* A live, impaired-fidelity coronavirus vaccine protects in an aged, immunocompromised mouse model of lethal disease. *Nat Med* 2012;18:1820–1826.
24. **Pfeiffer JK, Kirkegaard K.** Increased fidelity reduces poliovirus fitness and virulence under selective pressure in mice. *PLoS Path* 2005;1:e11.

25. **Sadeghipour S, McMinn PC.** A study of the virulence in mice of high copying fidelity variants of human enterovirus 71. *Virus Res* 2013;176:265–272.

26. **Ciota AT, Koch EM, Willsey GG, Davis LJ, Jerzak GV *et al.*** Temporal and spatial alterations in mutant swarm size of St. Louis encephalitis virus in mosquito hosts. *Infect Genet Evol* 2011;11: 460–468.

27. **Ciota AT, Lovelace AO, Ngo KA, Le AN, Maffei JG *et al.*** Cell-specific adaptation of two flaviviruses following serial passage in mosquito cell culture. *Virology* 2007;357:165–174.

28. **Shah NR, Sunderland A, Grdzelishvili VZ.** Cell type mediated resistance of vesicular stomatitis virus and Sendai virus to ribavirin. *PLoS One* 2010;5:e11265.

29. **Zeng J, Wang H, Xie X, Yang D, Zhou G *et al.*** An increased replication fidelity mutant of foot-and-mouth disease virus retains fitness *in vitro* and virulence *in vivo*. *Antiviral Res* 2013;100:1–7.

30. **Benarroch D, Egloff MP, Mulard L, Guerreiro C, Romette JL *et al.*** A structural basis for the inhibition of the NS5 dengue virus mRNA 2′-*O*-methyltransferase domain by ribavirin 5′-triphosphate. *J Biol Chem* 2004;279:35638–35643.

31. **Cassidy LF, Patterson JL.** Mechanism of La Crosse virus inhibition by ribavirin. *Antimicrob Agents Chemother* 1989;33:2009–2011.

32. **Goswami BB, Borek E, Sharma OK, Fujitaki J, Smith RA.** The broad spectrum antiviral agent ribavirin inhibits capping of mRNA. *Biochem Biophys Res Commun* 1979;89:830–836.

33. **Leyssen P, De Clercq E, Neyts J.** The anti-yellow fever virus activity of ribavirin is independent of error-prone replication. *Mol Pharmacol* 2006;69:1461–1467.

34. **Furuta Y, Takahashi K, Shiraki K, Sakamoto K, Smee DF *et al.*** T-705 (favipiravir) and related compounds: novel broad-spectrum inhibitors of RNA viral infections. *Antiviral Res* 2009;82:95–102.

35. **Lu G, Gong P.** Crystal structure of the full-length Japanese encephalitis virus NS5 reveals a conserved methyltransferase-polymerase interface. *PLoS Pathog* 2013;9:e1003549.

36. **Mosley RT, Edwards TE, Murakami E, Lam AM, Grice RL *et al.*** Structure of hepatitis C virus polymerase in complex with primer–template RNA. *J Virol* 2012;86:6503–6511.

37. **Brackney DE, Scott JC, Sagawa F, Woodward JE, Miller NA *et al.*** C6/36 *Aedes albopictus* cells have a dysfunctional antiviral RNA interference response. *PLoS Negl Trop Dis* 2010;4:e856.

38. **Rozen-Gagnon K, Stapleford KA, Mongelli V, Blanc H, Failloux AB *et al.*** Alphavirus mutator variants present host-specific defects and attenuation in mammalian and insect models. *PLoS Pathog* 2014;10:e1003877.

39. **Vignuzzi M, Stone JK, Andino R.** Ribavirin and lethal mutagenesis of poliovirus: molecular mechanisms, resistance and biological implications. *Virus Res* 2005;107:173–181.

40. **Vignuzzi M, Wendt E, Andino R.** Engineering attenuated virus vaccines by controlling replication fidelity. *Nat Med* 2008;14:154–161.

41. **Zeng J, Wang H, Xie X, Li C, Zhou G *et al.*** Ribavirin-resistant variants of foot-and-mouth disease virus: the effect of restricted quasispecies diversity on viral virulence. *J Virol* 2014;88:4008–4020.

42. **Graci JD, Cameron CE.** Mechanisms of action of ribavirin against distinct viruses. *Rev Med Virol* 2006;16:37–48.

43. **Arnold JJ, Vignuzzi M, Stone JK, Andino R, Cameron CE.** Remote site control of an active site fidelity checkpoint in a viral RNA-dependent RNA polymerase. *J Biol Chem* 2005;280: 25706–25716.

44. **Furuta Y, Takahashi K, Kuno-Maekawa M, Sangawa H, Uehara S *et al.*** Mechanism of action of T-705 against influenza virus. *Antimicrob Agents Chemother* 2005;49:981–986.

45. **Kiso M, Takahashi K, Sakai-Tagawa Y, Shinya K, Sakabe S *et al.*** T-705 (favipiravir) activity against lethal H5N1 influenza A viruses. *Proc Natl Acad Sci USA* 2010;107:882–887.

46. **Baranovich T, Wong SS, Armstrong J, Marjuki H, Webby RJ *et al.*** T-705 (favipiravir) induces lethal mutagenesis in influenza A H1N1 viruses *in vitro*. *J Virol* 2013;87:3741–3751.

47. **Brackney DE, Beane JE, Ebel GD.** RNAi targeting of West Nile virus in mosquito midguts promotes virus diversification. *PLoS Pathog* 2009;5:e1000502.

48. **Jerzak G, Bernard KA, Kramer LD, Ebel GD.** Genetic variation in West Nile virus from naturally infected mosquitoes and birds suggests quasispecies structure and strong purifying selection. *J Gen Virol* 2005;86:2175–2183.

49. **Ciota AT, Payne AF, Ngo KA, Kramer LD.** Consequences of *in vitro* host shift for St. Louis encephalitis virus. *J Gen Virol* 2014;95: 1281–1288.

50. **Gnadig NF, Beaucourt S, Campagnola G, Borderia AV, Sanz-Ramos M *et al.*** Coxsackievirus B3 mutator strains are attenuated *in vivo*. *Proc Natl Acad Sci USA* 2012;109:E2294–E2303.

51. **Greene IP, Wang E, Deardorff ER, Milleron R, Domingo E *et al.*** Effect of alternating passage on adaptation of Sindbis virus to vertebrate and invertebrate cells. *J Virol* 2005;79:14253–14260.

52. **Weaver SC, Brault AC, Kang W, Holland JJ.** Genetic and fitness changes accompanying adaptation of an arbovirus to vertebrate and invertebrate cells. *J Virol* 1999;73:4316–4326.

53. **Brackney DE, Schirtzinger EE, Harrison TD, Ebel GD, Hanley KA.** Modulation of flavivirus population diversity by RNA interference. *J Virol* 2015;89:4035–4039.

54. **Maharaj PD, Anishchenko M, Langevin SA, Fang Y, Reisen WK *et al.*** Structural gene (prME) chimeras of St Louis encephalitis virus and West Nile virus exhibit altered *in vitro* cytopathic and growth phenotypes. *J Gen Virol* 2012;93:39–49.

55. **Payne AF, Binduga-Gajewska I, Kauffman EB, Kramer LD.** Quantitation of flaviviruses by fluorescent focus assay. *J Virol Methods* 2006;134:183–189.

56. **Larkin MA, Blackshields G, Brown NP, Chenna R, McGettigan PA *et al.*** Clustal W and Clustal X version 2.0. *Bioinformatics* 2007;23: 2947–2948.

57. **Li H, Durbin R.** Fast and accurate long-read alignment with Burrows–Wheeler transform. *Bioinformatics* 2010;26:589–595.

58. **Li H, Handsaker B, Wysoker A, Fennell T, Ruan J *et al.*** The sequence alignment/map format and SAMtools. *Bioinformatics* 2009;25:2078–2079.